

# EXTREME DIVERGENCE AND ROTATION VALUES OF THE INERTIAL PARTICLE VELOCITY IN HIGH REYNOLDS NUMBER TURBULENCE USING DELAUNAY TESSELLATION

**Thibault Oujia**

Institut de Mathématiques de Marseille  
Aix-Marseille Université, CNRS  
Marseille, France  
thibault.oujia@univ-amu.fr

**Keigo Matsuda**

Research Institute for Value-Added  
Information Generation  
Japan Agency for Marine-Earth Science and Technology  
Yokohama, Japan  
k.matsuda@jamstec.go.jp

**Kai Schneider**

Institut de Mathématiques de Marseille  
Aix-Marseille Université, CNRS  
Marseille, France  
kai.schneider@univ-amu.fr

## ABSTRACT

The dynamics of inertial particles in homogeneous isotropic turbulence at high Reynolds number, obtained by three-dimensional direct numerical simulation (DNS), is analyzed considering different Stokes numbers. Divergence and rotation of the particle velocity are determined using Delaunay tessellation of the particle positions at subsequent time instants. For large Stokes numbers heavy tails in the probability density functions (PDFs) are found. Large divergence and rotation values, as large as 50 and 40 times of the corresponding standard deviation, respectively, can be observed. The helicity of the particle velocity, which quantifies the swirling motion of the particle flow, is likewise computed. The PDFs change their shape with the Stokes number and show that for large numbers higher probability for vanishing helicity is found. This confirms that for heavy particles helical motion is apparently suppressed.

## INTRODUCTION

Driven by numerous applications of particle laden turbulence, e.g. dust in stars or the rain formation in atmospheric clouds, there are many numerical and theoretical studies in the literature, see e.g. (Brownlee, 1985; Shaw, 2003). Understanding the motion of inertial particles is therefore essential to get insight into these phenomena and to develop sound models. The aim here is to determine the dynamical properties of inertial particles in isotropic turbulence using finite time tessellation-based measures. The particle velocity is crucial to understand particle dynamics, i.e. convergence, divergence of particles and the vortical or swirling motion of the particle clouds. The challenging task is that we only know the velocity of the particles at discrete points in space, i.e. at the particle position.

Voronoi tessellation of the particle position has previously been used, e.g. in Monchaux *et al.* (2010), for analyzing preferential concentration of inertial particles. In our recent work,

Oujia *et al.* (2020), we proposed a Lagrangian approach to determine the divergence of particle velocity using the volume change rate of the Voronoi cells. Here we propose a further new Lagrangian approach using Delaunay tessellation, to determine the spatial velocity derivatives numerically by considering subsequent time instants. In particular the trace of the velocity gradient tensor, corresponding to the divergence, which yields information about sources and sinks and its antisymmetric part, corresponding to the curl, which characterizes the rotation can thus be computed. The helicity, i.e. the scalar product of vorticity and velocity, can be likewise calculated and swirling motion of particle clouds can consequently be quantified. The dynamical properties of the particle velocity can be assessed and detailed statistics of the divergence and of the rotation can be performed.

Moreover, we will address the presence of extreme values in these quantities which is reflected in heavy tails in the probability distribution functions (PDFs). Extreme events are a generic feature of turbulence, see e.g., Moffatt (2021), and make its prediction particularly difficult, e.g., for tornadoes, large floods and other extreme events with devastating impact. In the present work we will show that the divergence and rotation values of the particle velocity likewise have extreme intensities, much larger than their standard deviation.

The remainder of the manuscript summarizes first the DNS flow data we analyze. Then we describe the method to determine the divergence and rotation based on Delaunay tessellation of the particle positions. Numerical results and extreme divergence and rotation values are presented afterwards and finally some conclusions are drawn.

## FLOW DATA AND METHODS

Particle position and velocity data are generated by DNS of particle-laden homogeneous isotropic turbulence, presented in Matsuda *et al.* (2014). The incompressible Navier-Stokes equations are solved in a  $2\pi$ -periodic cube with a fourth order finite difference scheme. Statistically stationary flow is obtained by forcing at large scales. Uniformly distributed dis-

crete particles are then injected into the fully developed flow and are tracked in the Lagrangian framework. Maxey's model (Maxey, 1987) for inertial heavy point particles with Stokes drag is used and the inertial dynamics is controlled by the Stokes number,  $St = \tau_p / \tau_\eta$ , where  $\tau_p$  is the particle relaxation time and  $\tau_\eta$  the Kolmogorov time. The equation of particle velocity  $\mathbf{v}_{pj}$  is given by

$$d_t \mathbf{v}_{pj} = - \frac{\mathbf{v}_{pj} - \mathbf{u}_{pj}}{\tau_p}, \quad (1)$$

where  $\mathbf{u}_{pj}$  is the fluid velocity at particle position  $\mathbf{x}_{pj}$ . The subscript  $p$  denotes the quantity at the position of a particle, and the subscript  $j$  denotes the particle identification number.

State of the art high resolution DNS with  $N_g^3 = 512^3$  grid points is performed for the Taylor-microscale Reynolds number  $Re_\lambda = 204$ , where  $Re_\lambda \equiv u' \lambda / \nu$ ,  $\nu$  is the kinematic viscosity, and  $\lambda$  is the Taylor microscale. The number of particles  $N$  is  $1.5 \times 10^7$  and the considered Stokes numbers are  $St = 0.5, 1, 2$  and  $5$ . Particles with different Stokes numbers, including  $St = 0$  were tracked in an identical turbulent flow.

We apply 3D Delaunay tessellation (Delaunay, 1934) using the Quickhull algorithm (Barber *et al.*, 1996) to the particle positions at two consecutive time instants. To define a cell corresponding to a particle, we use the dual graph of the Delaunay tessellation. For stability reasons, instead of using the circumcenter of the Delaunay cell, as done for the Voronoi tessellation, we use the center of gravity to define the vertices of the cell.

To compute the divergence of the particle velocity  $\mathcal{D}(\mathbf{v}_p)$ , we consider the local number density averaged over a cell, which is the inverse of the corresponding volume. Using the fact that particles satisfy the conservation equation of the density  $n_p$ ,  $D_t n_p = -n_p \nabla \cdot \mathbf{v}_p$  where  $D_t = \partial_t + \mathbf{v} \cdot \nabla$  is the Lagrangian derivative and considering two time instants  $t^k$  and  $t^{k+1} = t^k + \Delta t$  of the Delaunay tessellation with time step  $\Delta t$ , we can determine the volume change. Thus we obtain (Oujia *et al.*, 2020),

$$\mathcal{D}(\mathbf{v}_p) = - \frac{1}{n_p} D_t n_p = \frac{2}{\Delta t} \frac{V_p^{k+1} - V_p^k}{V_p^{k+1} + V_p^k} \quad (2)$$

The curl of the particle velocity, is defined by computing the circulation of the velocity field of particles over a cell. This can also be expressed as the divergence of the velocity of the fluid which has been rotated in a direction  $\pi/2$  with respect to the direction of the curl. We define  $\mathbf{v}_x^\perp = A_x \mathbf{v}$ ,  $\mathbf{v}_y^\perp = A_y \mathbf{v}$  and  $\mathbf{v}_z^\perp = A_z \mathbf{v}$  where  $A_x$ ,  $A_y$  and  $A_z$  are rotation matrices around the different axes. We obtain that the curl of the particle velocity  $\mathcal{C}(\mathbf{v}_p)$  is given by

$$\mathcal{C}(\mathbf{v}_p) = \begin{pmatrix} \mathcal{D}(-\mathbf{v}_{p,x}^\perp) \\ \mathcal{D}(-\mathbf{v}_{p,y}^\perp) \\ \mathcal{D}(-\mathbf{v}_{p,z}^\perp) \end{pmatrix} \quad (3)$$

The accuracy and reliability of the method to compute the divergence, curl and furthermore the velocity gradient tensor of the particle velocity are studied in Oujia *et al.* (2022). We find that the spatial order of the method is the inverse of the dimension of the space.

## RESULTS

Figure 1 shows two-dimensional cuts of the particles colored with the divergence  $\mathcal{D}(\mathbf{v}_p)$  (top) and the enstrophy  $\|\mathcal{C}(\mathbf{v}_p)\|_2^2$  (bottom) for  $St = 0$  (left) and  $1$  (right). The particles for  $St = 0$ , i.e. fluid particles, are randomly distributed because the flow is incompressible. We can deduce that for  $St = 0$  the divergence values different from zero are numerical errors due to the sampling. Their distribution is homogeneous and we find mostly values close to zero, except in some regions, which are characterized by strong enstrophy values. The enstrophy of the fluid particles (bottom, left) shows a non homogeneous distribution and is spotty, characteristic for intermittent quantities. In contrast to fluid particles, inertial particles (Figure 1, right), here for  $St = 1$ , are clustered. We can observe the preferential concentration of particles, corresponding to clusters in regions of low fluid vorticity and voids in regions of large fluid vorticity. This observation is explained by the fact that inertial particles are ejected from high fluid vorticity regions due to the centrifugal force. We also find the high convergence and divergence value are observed close to each other. We conjecture that the particles are crossing. In a sufficiently large region of low fluid vorticity, we can observe that divergence and enstrophy values of inertial particles are close to zero.

PDFs of divergence and rotation are shown in Figure 2. As the turbulence is isotropic, we do not distinguish between the different vector components of  $\mathcal{C}(\mathbf{v}_p)$ , and we compute the histograms of all these components together. For fluid particles in the continuous setting, the divergence of the fluid velocity vanishes exactly, whereas in the discrete setting  $\mathcal{D}(\mathbf{v}_p)$  differs from zero due to the sampling and the computation of the discrete divergence. For inertial particles, the PDFs of the divergence and of the rotation deviate from those for fluid particles. This nicely illustrates that for large Stokes numbers heavy tails and extreme values can be observed in both quantities, going up to more than 50 and 40 times of the standard deviation for the divergence and the rotation, respectively. The PDFs of the divergence and of the rotation have much heavier tails compared to the fluid vorticity, and the extreme values increase significantly with the Stokes number. This is quantified further in Table 1, where each of the variance and flatness of the divergence  $\mathcal{D}(\mathbf{v}_p)$  and curl  $\mathcal{C}(\mathbf{v}_p)$  is given as a function of the Stokes number. We observe that the variance of the divergence increases as the Stokes number increases. The flatness of the divergence first increases with  $St$  with a maximum for  $St = 1$  and then decreases. The large flatness value is a sign of strong non-Gaussianity and the spatially intermittent behavior of the divergence for  $St = 1$ . These observations suggest that the global number of particles with large divergence values increases with the Stokes number. Note that for  $St > 1$  tails become shallower with increasing  $St$  when the PDFs are normalized by the standard deviation, not shown here. We recall that the divergence of the particles is induced by the vorticity of the fluid flow via the centrifugal force. The decay of the flatness for  $St \geq 2$  can be explained by the particle's inertia. In fact, heavy particles are less subjected to the small scale fluctuations of the fluid vorticity, so that the particles follow less the fluid flow and thus have less tendency to accelerate suddenly. The variance of the curl decreases from  $St = 0$  to  $0.5$  and then increases as the Stokes number increases. The flatness decreases from  $St = 0$  to  $0.5$  and then increases with  $St$  with a maximum for  $St = 2$  and then decreases. The reduction of the variance and flatness of the curl between  $St = 0$  and  $0.5$  can be explained by the fact that the particles in the high velocity regions in the fluid domain are ejected due to the centrifugal force. However, for a small  $St$  the particle velocity

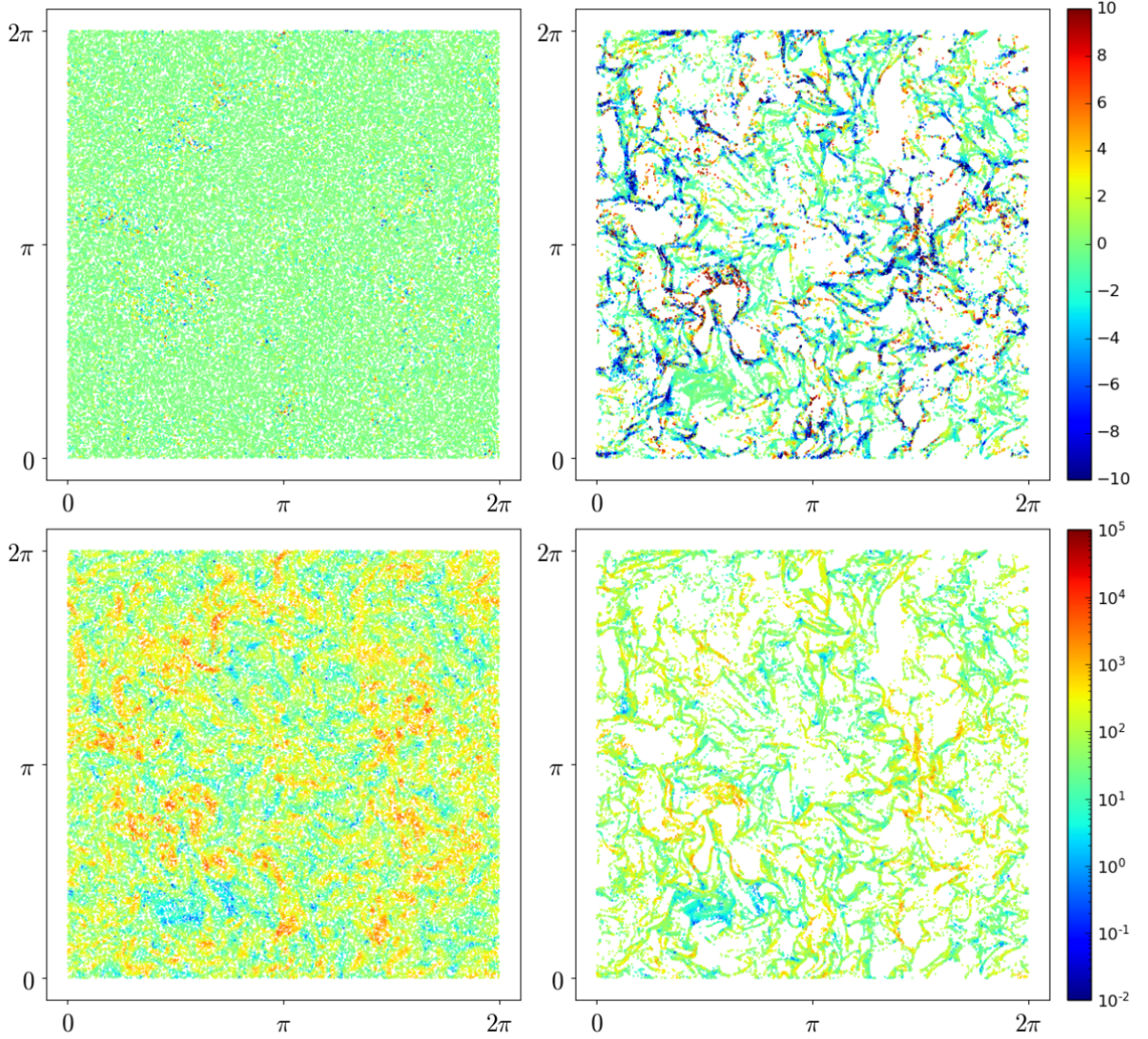


Figure 1: Spatial distribution of the particles colored with the divergence  $\mathcal{D}(\mathbf{v}_p)$  (top) and the enstrophy  $\|\mathcal{E}(\mathbf{v}_p)\|_2^2$  (bottom) at particles positions for  $St = 0$  (left) and 1 (right) for a slice of thickness  $4\eta$ . Note that the color scale is linear for the divergence and logarithmic for the enstrophy.

at a given position is still close to that of the fluid. This explains the reduction of the curl value between  $St = 0$  and 0.5 as well as that of the variance. The increase of the variance of the curl value for larger Stokes numbers could be explained by the higher inertia. Due to the sling effect, the particle trajectories may cross each other, or the particles may enter high vorticity regions and experience strong vortical motion.

Figure 3 shows the PDF of the relative helicity of particle velocity for different Stokes numbers and randomly distributed particles. The relative helicity of the particle velocity is defined as

$$\mathcal{H}(\mathbf{v}_p) = \frac{\mathbf{v}_p \cdot \mathcal{E}(\mathbf{v}_p)}{\|\mathbf{v}_p\|_2 \|\mathcal{E}(\mathbf{v}_p)\|_2} \quad (4)$$

We can observe that for  $St \leq 1$  there are two maxima at  $\mathcal{H}_p = \pm 1$ , which means that we have a higher probability that the vorticity is oriented in the same or opposite direction as the particle velocity. This corresponds to helical motion, which is

a signature of coherent structures in the particle laden flow. In contrast we find for  $St = 5$  two minima at  $\mathcal{H}_p = \pm 1$  and a maximum close to 0 which means that the vorticity has higher probability to be orthogonal to the particle velocity, which indicates incoherent particle flow motion. We can observe a transition from a convex to a concave shape at  $St = 2$ . Note that the asymmetry of the distribution can be explain by the presence of helicity asymmetry in the fluid flow due to initial forcing.

## CONCLUSIONS

We analyzed high resolution DNS data of particle laden turbulence considering different Stokes numbers. We proposed a semi-Lagrangian method to determine the divergence and rotation of the particle velocity. To this end we considered the time change of the Delaunay tessellation of the particle positions and computed the spatial derivatives in the Lagrangian frame. Consequently the divergence, the curl and likewise the helicity of the particle motion could be quantified. We showed that the divergence and curl PDFs exhibit heavy

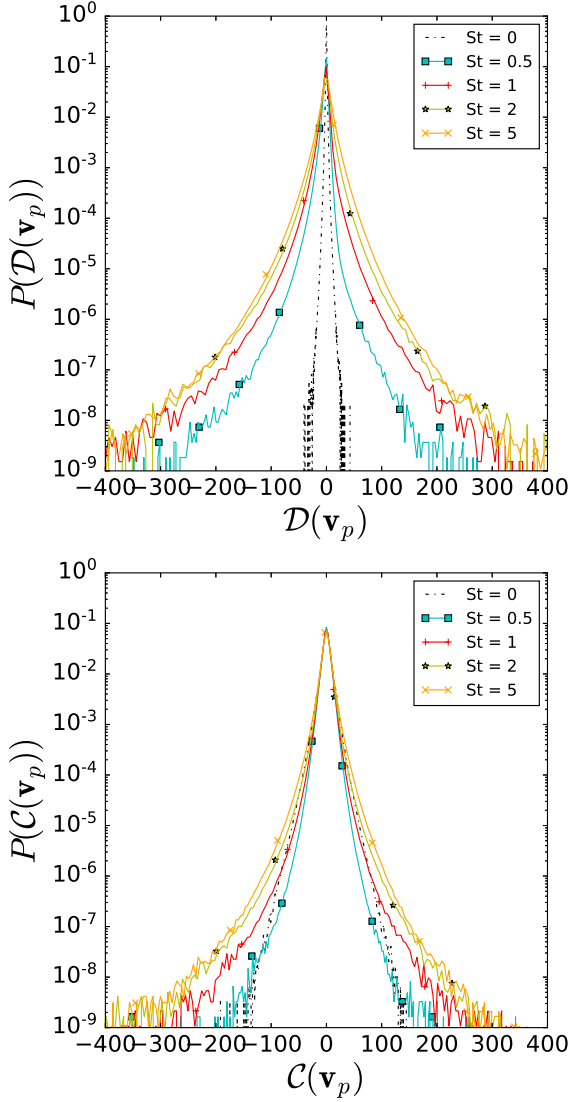


Figure 2: PDFs of divergence  $\mathcal{D}_p$  (top) and rotation  $\mathcal{C}_p$  (bottom) for the particle velocity for different Stokes numbers including fluid particles.

Table 1: Variance  $\mathbb{V}$  and flatness  $\mathbb{F}$  of divergence  $\mathcal{D}_p$  and curl  $\mathcal{C}_p$  as a function of the Stokes number.

St	0	0.5	1	2	5
$\mathbb{V}(\mathcal{D}_p)$	0.87	16.9	43.8	88.5	152
$\mathbb{F}(\mathcal{D}_p)$	15.9	55.3	64.0	33.5	15.8
$\mathbb{V}(\mathcal{C}_p)$	68.8	42.7	49.7	60.1	82.3
$\mathbb{F}(\mathcal{C}_p)$	7.83	7.02	12.0	17.7	14.9

tails and we found that for large Stokes numbers extreme values are above 40 times the corresponding standard deviations. In future work, we plan to perform multiscale analysis using multiresolution tessellations.

ACKNOWLEDGEMENTS: T.O. and K.S. acknowledge partial funding from the Agence Nationale de la Recherche (ANR), grant ANR-20-CE46-0010-01. Centre de Calcul Intensif d’Aix-Marseille is ac-

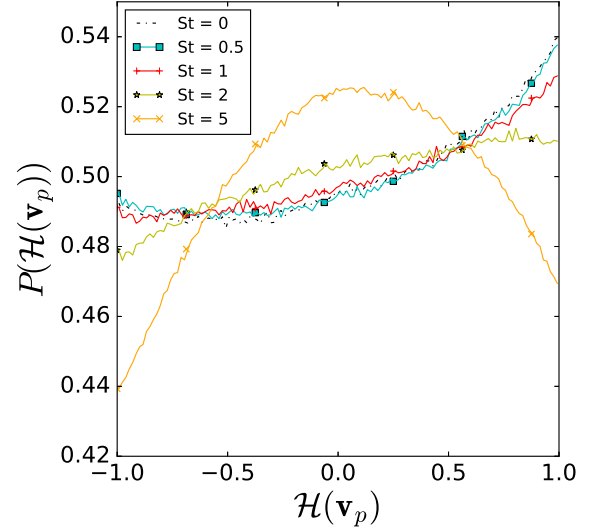


Figure 3: PDFs of the relative helicity (cosine of the angle between velocity and vorticity)  $\mathcal{H}_p$  of the particles for different Stokes numbers including fluid particles ( $St = 0$ ).

knowledgeled for granting access to its high performance computing resources. K.M. acknowledges financial support from JSPS KAKENHI Grant Number JP20K04298. The DNS data analysed in this project were obtained using the Earth Simulator supercomputer system of JAMSTEC.

## REFERENCES

- Barber, C. B., Dobkin, D.P. & Huhdanpaa, H.T. 1996 The quickhull algorithm for convex hulls, *acm transactions on mathematical software*. *ACM Trans. Math. Software (TOMS)* **22** (4), 469–483.
- Brownlee, Donald E 1985 Cosmic dust: Collection and research. *Annual Review of Earth and Planetary Sciences* **13** (1), 147–173.
- Delaunay, B. 1934 Sur la sphère vide. *Izv. Akad. Nauk SSSR, Otdelenie Matematicheskii i Estestvennyka Nauk* **7** (793–800), 1–2.
- Matsuda, K., Onishi, R., Hirahara, M., Kurose, R., Takahashi, K. & Komori, S. 2014 Influence of microscale turbulent droplet clustering on radar cloud observations. *J. Atmos. Sci.* **71** (10), 3569–3582.
- Maxey, M. R. 1987 The gravitational settling of aerosol particles in homogeneous turbulence and random flow fields. *J. Fluid Mech.* **174**, 441–465.
- Moffatt, HK 2021 Extreme events in turbulent flow. *Journal of Fluid Mechanics* **914**.
- Monchaux, R., Bourgoin, M. & Cartellier, A. 2010 Preferential concentration of heavy particles: a voronoi analysis. *Phys. Fluids* **22** (10), 103304.
- Oujia, Thibault, Matsuda, Keigo & Schneider, Kai 2020 Divergence and convergence of inertial particles in high-reynolds-number turbulence. *Journal of Fluid Mechanics* **905**, A14.
- Oujia, Thibault, Matsuda, Keigo & Schneider, Kai 2022 Differential operators using volume change of tessellation cells. *Preprint*.
- Shaw, R. A. 2003 Particle-turbulence interactions in atmospheric clouds. *Annu. Rev. Fluid Mech.* **35** (1), 183–227.